

15-Lipoxygenase Catalytically Consumes Nitric Oxide and Impairs Activation of Guanylate Cyclase*

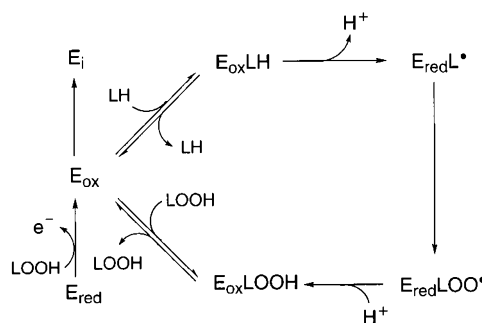
(Received for publication, November 25, 1998, and in revised form, March 27, 1999)

Valerie B. O'Donnell^{‡§}, Kenneth B. Taylor[¶], Sampath Parthasarathy[¶], Hartmut Kühn^{**}, Doris Koesling^{‡‡}, Andreas Friebe^{‡‡}, Allison Bloodsworth^{‡§}, Victor M. Darley-USmar^{§ §§}, and Bruce A. Freeman^{‡§ ¶¶}

From the Departments of [‡]Anesthesiology, [¶]Biochemistry and Molecular Genetics, and ^{§§}Pathology and the [§]Center for Free Radical Biology, University of Alabama at Birmingham, Birmingham, Alabama 35233, the ^{¶¶}Department of Obstetrics and Gynecology, Emory University, Atlanta, Georgia 30322, the ^{**}Institute of Biochemistry, Humboldt University, Hessische Strasse 3-4 Berlin, Germany, and the ^{‡‡}Institute of Pharmacology, Freie University, Thielalle 69-73 Berlin, Germany

Analysis of purified soybean and rabbit reticulocyte 15-lipoxygenase (15-LOX) and PA317 cells transfected with human 15-LOX revealed a rapid rate of linoleate-dependent nitric oxide (NO) uptake that coincided with reversible inhibition of product ((13S)-hydroperoxyoctadecadienoic acid, or (13S)-HPODE) formation. No reaction of NO (up to 2 μ M) with either native (E_{red}) or ferric LOXs (0.2 μ M) metal centers to form nitrosyl complexes occurred at these NO concentrations. During HPODE-dependent activation of 15-LOX, there was consumption of 2 mol of NO/mol of 15-LOX. Stopped flow fluorescence spectroscopy showed that NO (2.2 μ M) did not alter the rate or extent of (13S)-HPODE-induced tryptophan fluorescence quenching associated with 15-LOX activation. Additionally, NO does not inhibit the anaerobic peroxidase activity of 15-LOX, inferring that the inhibitory actions of NO are due to reaction with the enzyme-bound lipid peroxyl radical, rather than impairment of (13S)-HPODE-dependent enzyme activation. From this, a mechanism of 15-LOX inhibition by NO is proposed whereby reaction of NO with $E_{red}LOO^{\bullet}$ generates E_{red} and LOONO, which hydrolyzes to (13S)-HPODE and nitrite (NO_2^-). Reactivation of E_{red} , considerably slower than dioxygenase activity, is then required to complete the catalytic cycle and leads to a net inhibition of rates of (13S)-HPODE formation. This reaction of NO with 15-LOX inhibited NO-dependent activation of soluble guanylate cyclase and consequent cGMP production. Since accelerated NO production, enhanced 15-LOX gene expression, and 15-LOX product formation occurs in diverse inflammatory conditions, these observations indicate that reactions of NO with lipoxygenase peroxyl radical intermediates will result in modulation of both NO bioavailability and rates of production of lipid signaling mediators.

heme iron-containing enzymes that oxidize the unsaturated fatty acids arachidonate and linoleate to bioactive hydroperoxides and other metabolites (Scheme 1). For example, 5-LOX¹



SCHEME 1. Dioxygenase cycle of 15-LOX. Ferrous enzyme (E_{red}) is oxidized by peroxide product ($LOOH$), forming ferric enzyme with bound hydroperoxide product (E_{ox}). Lipid substrate (LH) binds E_{ox} , becoming oxidized to yield reduced enzyme with bound lipid alkyl radical ($E_{red}L^{\bullet}$). Following rearrangement of the alkyl radical to a conjugated diene, oxygen is stereospecifically inserted, forming reduced enzyme with bound lipid peroxyl radical ($E_{red}LOO^{\bullet}$). Following reduction of the peroxyl radical by the reduced enzyme, the ferric enzyme is regenerated ($E_{ox}LOOH$), and the peroxide product ($LOOH$) dissociates. During dioxygenase turnover, rabbit but not soybean 15-LOX self-inactivates (E_i).

generates precursors for leukotrienes, products involved in inflammation and allergic responses (1). 12-Lipoxygenases, present in vascular endothelium, smooth muscle cells, platelets, and leukocytes (2, 3), contribute to vascular cell hypertrophy, proliferation, and hypertensive actions, while 15-LOX is involved in cell development and differentiation, particularly in reticulocytes where 15-LOX oxidation of mitochondrial phospholipids is a trigger for their degradation (2, 4, 5).

A central pathogenic role for 15-LOX in atherosclerosis comes from multiple lines of evidence, in particular the colocalization of 15-LOX mRNA, enzymatic activity, and the relatively specific pattern of isomeric 15-LOX oxygenation products that have been detected in early human and rabbit lesions (6–9). The accumulation and oxidation of low density lipoprotein (LDL) lipids by monocytes and the subsequent accumulation of oxidized lipids and foam cells in the vascular intima is a hallmark of early atherogenesis. *In vitro* studies have shown

Lipoxygenases are a family of ubiquitously expressed non-

* This work was supported by National Institutes of Health Grants P60-HL58418, P01-HL40456, R01-HL51245 (to B. A. F. and V. D. U.), and R01-HL52628 (to S. P.); by a grant from the Parker B. Francis Foundation (to V. B. O.); and by Deutsche Forschungsgemeinschaft Grant Kn 961/2-2 (to H. K.). The costs of publication of this article were defrayed in part by the payment of page charges. This article must therefore be hereby marked "advertisement" in accordance with 18 U.S.C. Section 1734 solely to indicate this fact.

¶¶ To whom all correspondence should be addressed: Dept. of Anesthesiology, 946 THF, 619 19th St. S., University of Alabama at Birmingham, Birmingham, AL 35233. Fax: 205-934-7437; E-mail: bruce.freeman@ccc.uab.edu.

¹ The abbreviations used are: LOX, lipoxygenase; LDL, low density lipoprotein; HPLC, high performance liquid chromatography; PBS, phosphate-buffered saline; HPODE, hydroperoxyoctadecadienoic acid; ETYA, eicosatetraynoic acid; DTPA, diethylenetriamine pentaacetic acid; DEA-NONOate, 2-(N,N-diethylamino)-diazeneolate-2-oxide.

that macrophage and endothelial cell lipoxygenases readily oxidize externally added LDL and promote metal-dependent lipoprotein oxidation (10–12). *In vivo* models show that somatic gene transfer of 15-LOX to vessels and transgenic mice cross-bred with LDL receptor-deficient mice results in increased oxidation of LDL and accumulation of lipid-containing vascular lesions (13, 14). A currently provocative counterpoint to these properties of 15-LOX is the observation that targeted overexpression of rabbit macrophage 15-LOX prevented diet-induced atherosclerosis (15). In contrast, diet-induced atherosclerosis in rabbits is inhibited by administration of a 15-LOX inhibitor having limited direct antioxidant properties (16). In aggregate, these observations encourage better understanding of the interactions of 15-LOX, 15-LOX products, and vascular cells with key mediators of vascular function and atherogenesis, in particular NO.

In vitro, NO can act as a potent antioxidant by scavenging lipid-derived peroxy and alkoxyl radicals formed in purified or LDL lipids oxidized by Cu^{2+} , azo initiators, peroxynitrite (ONOO^-), endothelial cells or macrophages (17–24). Inhibition of both plant and mammalian 15-LOX-dependent lipid oxidation by high concentrations of nitric oxide (NO) was ascribed to formation of an enzyme-nitrosyl complex (25–27). Nitric oxide can form a nitrosyl complex with the active site of 15-LOX, a single six-coordinate ferrous iron liganded to nitrogen and/or oxygen atoms (28), that is detectable by electron paramagnetic resonance spectroscopy (EPR). The spectrum of the soybean 15-LOX Fe^{2+} -NO complex contains two species, the first attributed to either high spin ferric iron, formed by transfer of an electron from Fe^{2+} to NO, or an $S = 3/2$ system resulting from antiferromagnetic coupling of axial ($D > E$) high spin ferrous iron to NO (29–31). The dissociation constant (K_d) for formation of this species is 95 μM for soybean 15-LOX at pH 7 (31). The second component of the EPR spectra has been suggested to be a high spin Fe^{2+} -NO complex and requires NO concentrations of at least 400 μM for detection (30). Three lines of evidence suggested that oxidation of the reduced iron by NO, leading to enzyme activation, might occur following formation of the nitrosyl complex. Addition of NO to anaerobic ferrous 15-LOX resulted in immediate appearance of a pale yellow color, identical to that of the ferric enzyme found on treating native enzyme with HPODE (29). Additionally, EPR and x-ray absorption analysis of rabbit 15-LOX showed that incubation with millimolar concentrations of NO yielded ferric iron species (25). Importantly, the NO concentrations required for formation of the Fe^{2+} -NO complex significantly exceed those (a) required to inhibit soybean 15-LOX catalytic activity (32) and (b) maximal NO levels typically found in biological systems, typically <1–5 μM (33–34), suggesting that 15-LOX inhibition does not involve Fe^{2+} -NO complex formation. Thus, other mechanisms are likely to be operative in the NO-mediated inhibition of lipoxygenase-dependent lipid oxidation.

In addition to the ferrous iron, several species form during 15-LOX catalysis that could potentially react with NO and lead to enzyme inhibition. These include enzyme-bound lipid peroxy, alkoxyl, and carbon-centered radicals. Termination reactions of NO with non-lipid-derived radicals are fast, occurring at essentially diffusion-limited rates (35, 36). In addition, kinetic studies indicate that NO also reacts extremely rapidly with lipid-derived radicals in aqueous systems (18, 22, 36). Since NO can diffuse into the 15-LOX active site, we hypothesized that enzyme-bound lipid-derived radicals are accessible to NO during turnover.

In biological systems, efficient removal of NO following its synthesis by nitric oxide synthases is critical in maintaining control of vascular tone. While oxyhemoglobin, present in

erythrocytes, reacts with and removes NO in the vascular space (37), little is known regarding the processes that remove NO in the subendothelial compartment. The half-life of NO in hemoglobin-free cascade bioassays is only 3–5 s (38), far too short to be accounted for by simple autoxidation, suggesting that cell-dependent NO consumption also occurs. Under pathological conditions NO consumption becomes excessive, with complete loss of the pathways dependent upon activation of soluble guanylate cyclase (39). One component of the inhibition of the NO signaling is the reaction of endothelial-derived relaxation factor with superoxide (O_2^-) to yield peroxynitrite (ONOO^-) (39–42). Since reactions of O_2^- do not account for complete loss of NO signaling to smooth muscle cells (42), other unidentified metabolic pathways that contribute to NO consumption are inferred. Such an alternative are the free radical intermediates populated during the turnover of enzymes mediating electron transfer reactions. During development of diet-induced atherosclerosis in rabbits, impairment of the vascular response to endothelial-derived relaxation factor or NO is a consistent finding (40–42). Since 15-LOX is known to be present in the subendothelial layer in atherosclerotic lesions and NO can concentrate in lipophilic milieu (33), it was of interest to investigate whether reactions of lipid radicals generated by 15-LOX can proceed at a significant enough rate to alter cellular NO levels and impact on NO-dependent signaling.

Herein, the reactions of soybean and mammalian 15-LOX with NO at concentrations encompassing those found under physiological and pathological conditions were examined. Our results indicate that there are two distinct sites for NO reaction during 15-LOX catalysis, and that NO consumption occurs during inhibition of 15-LOX. It was also observed that, during 15-LOX catalysis of lipid oxidation, lipid radical reactions with NO in turn inhibited NO-mediated activation of soluble guanylate cyclase and the subsequent formation of cGMP. In aggregate, these observations reveal that lipoxygenase reactions with NO can inhibit both lipoxygenase catalytic activity and NO-dependent signal transduction.

EXPERIMENTAL PROCEDURES

Materials—Rabbit reticulocyte 15-LOX was purified to electrophoretic homogeneity from the lysate of a reticulocyte-rich blood cell suspension by fractionated ammonium sulfate precipitation and two consecutive steps of fast liquid protein chromatography (43). Soluble guanylyl cyclase was purified from bovine lung to homogeneity by immunoaffinity chromatography as previously (29). Linoleic acid was from Nu-Chek Prep (Elysian, MN). Unless stated otherwise, all enzymes and chemicals, including soybean 15-LOX type V was purchased from Sigma.

Culture of 15-LOX-transfected PA317 Cells—Murine PA317 fibroblasts stably transfected with either pLLORN or pLZRNL (44) were maintained in Dulbecco's modified Eagle's medium supplemented with 10% fetal bovine serum supplemented with glutamine and antibiotics. The plasmids pLLORN and pLZRNL are derived from the retroviral vector, pLDRNL, where the LDL receptor cDNA sequence has been replaced with either human 15-LOX cDNA or β -galactosidase cDNA (lacZ), respectively (44, 45). The 15-LOX transfectants are designated clone 12 and have been derived by clonal selection of the pLLORN-transfected cells, and possess 10–20-fold greater 15-LOX specific activity than the lacZ-infected controls (43).

Synthesis of (13S)-Hydroperoxyoctadecadienoic acid ((13S)-HPODE)—(13S)-Hydroperoxyoctadecadienoic acid ((13S)-HPODE) was synthesized as described (46). Product analysis using both normal and chiral phase HPLC (see "HPLC Analysis of Reaction Products" for details) indicated HPODE products were 97% (13S)-HPODE and 3% (13R)-HPODE.

15-LOX Assay Systems—To accurately determine enzyme concentrations, titrations with (13S)-HPODE were monitored fluorimetrically, where quenching of intrinsic tryptophan fluorescence during activation is mediated by 1 mol of HPODE/mol of enzyme (47). 15-LOX activity was assayed spectrophotometrically at 234 for conjugated diene forma-

tion ($E_{234\text{ nm}} = 28\text{ mM}^{-1}\text{ cm}^{-1}$). 15-LOX assay was performed at 20 °C or 37 °C for the soybean and rabbit enzymes, respectively, with stirring. The assay mixture was 2 ml 0.1 M potassium phosphate buffer (pH 7.4), 0.5 mM linoleic acid, 100 mM diethylenetriaminepentaacetic acid (DTPA), and 0.2% sodium cholate (48). 15-LOX-catalyzed hydroperoxidase activity was determined as oxodienone formation at 280 nm.

Measurement of Nitric Oxide Uptake—Anaerobic solutions of 1.9 μM NO were prepared by equilibrating NO gas (Matheson, Madison, WI) in argon-saturated deionized water. Any NO₂ present was eliminated by first bubbling NO through 5 M NaOH. Nitric oxide was measured by electrochemical detection using a NO sensor (Iso-NO, WPI Inc., Sarasota, FL). Electrode response calibration was done by measuring NO liberated from 50 μM KNO₂, 0.1 M KI, and 0.1 M H₂SO₄, using the following reaction performed under anaerobic conditions: $2\text{KNO}_2 + 2\text{KI} + 2\text{H}_2\text{SO}_4 \rightarrow 2\text{NO} + \text{I}_2 + 2\text{H}_2\text{O} + 2\text{K}_2\text{SO}_4$ (as per the instruction manual). For measurement of NO consumption by 15-LOX, NO (1–5 μM) was added to sample buffer containing linoleate without enzyme. Once the electrode response had stabilized, enzyme was added and rates of NO consumption recorded. For measurement of NO consumption by PA317 cells, monolayers were trypsinized, washed, counted, then kept at 5 °C in PBS, pH 7.4. For assay, $1\text{--}2 \times 10^6$ cells were added to 1 ml of PBS in the chamber of the NO electrode, at 37 °C with stirring. Nitric oxide (1.9 μM) was added and consumption rates monitored with or without addition of 0.5 mM linoleate. In some experiments, cells were preincubated with 100 μM eicosatetraynoic acid (ETYA) for 10 min at 37 °C before addition of NO and linoleate. Fatty acids were added in ethanol with final concentration less than 0.5%.

Measurement of Soluble Guanylate Cyclase Activation—Guanylate cyclase activity was measured by conversion of [α -³²P]GTP to [α -³²P]cGMP at 37 °C for 1 min. Reaction mixtures contained 92 ng of soluble guanylate cyclase, 3 mM MgCl₂, 1 mM cGMP, 0.3 mM [α -³²P]GTP ($\sim 3 \times 10^5$ cpm) in 0.1 ml of 50 mM triethanolamine/HCl buffer, pH 7.4. In some reactions, samples also contained 5 μM arachidonate and/or rabbit 15-LOX (1.3 nM). Reactions were initiated by adding DEA-NONOate (0.5 μM) and transferring complete reaction systems from 4 °C to 37 °C. In some reactions, 15-LOX was added at the same time as DEA-NONOate. Reactions were terminated by ZnCO₃ precipitation, followed by isolation of [α -³²P]cGMP as previously (49). Results were corrected for enzyme-deficient blanks and recovery of cGMP.

Sample Preparation for Analysis of Lipid Oxidation and Nitration Products—In these experiments, 0.1 mM linoleic acid was used to ensure that lipid substrate was consumed before oxygen was depleted, thus preventing anaerobic hydroperoxidase activity. Nitric oxide (7.6 μM) was added to 0.1 mM linoleate, 100 μM DTPA, and 0.2% sodium cholate, pH 7.4, in 2 ml of phosphate buffer. Then soybean LOX was added, and NO consumption rates monitored. As NO approached zero, further 7.6 μM additions were made. When all linoleate was consumed, NO uptake slowed and samples were immediately removed and placed on ice until extraction of lipids for HPLC analysis. Controls were prepared by allowing 15-LOX to oxidize 100 μM linoleate in the absence of NO.

Leukomethylene Blue Assay for Hydroperoxides—Sample (50 μl) was added to 100 μl of leukomethylene blue reagent (5 mg of leukomethylene blue, 8 ml of dimethylformamide, 1.4 g of Triton X-100, 5.5 mg of hemoglobin in 100 ml of 0.05 M potassium phosphate buffer, pH 5.0) and absorbance measured at 650 nm using a microplate reader (50).

HPLC Analysis of Reaction Products—Contaminating NO₂[−] was removed by adding equal volumes of 1% sulfanilamide, 3 N HCl, and 0.02% *N*-(1-naphthyl)-ethylenediamine to samples. Following this, lipids were twice-extracted with two volumes of diethyl ether. Extracts were dried over sodium sulfate (30 min, 4 °C) and the solvent evaporated with a stream of nitrogen. Lipids were reconstituted in 0.2 ml of methanol and stored at −80 °C under nitrogen atmosphere. Reversed-phase HPLC was carried out on a 150 mm \times 4.6 mm, *i.e.* 5- μm C₁₈ column (Microsorb, Rainin, MA) using a gradient of 50% B to 90% B over 20 min (A: water:acetonitrile:acetic acid, 75:25:0.1, v/v; B: methanol:acetonitrile:acetic acid, 60:40:0.1, v/v) at 1 ml/min. Absorbance was monitored at 235 nm (conjugated dienes) and 205 nm (linoleic acid). Products were identified and quantified using (13S)-HPODE, with standard curves linear over the concentration range examined, and between-day variation at 6%. Normal phase high pressure liquid chromatography (NP-HPLC) was carried out on a Spherisorb S5W column (Phase-Sep 250 \times 4.6 mm, 5- μm particle size) eluted with *n*-hexane:2-propanol:acetic acid, 100:2:0.1, v/v at 1 ml/min. For determination of HPODE enantiomer composition, a Chiralcel OD column (J.T. Baker, 250 \times 4.6 mm, 5- μm particle size) was used with *n*-hexane:2-propanol:acetic acid, 100:2:0.1, v/v, at 1 ml/min.

Liquid Chromatography-Mass Spectrometry—To examine for ni-

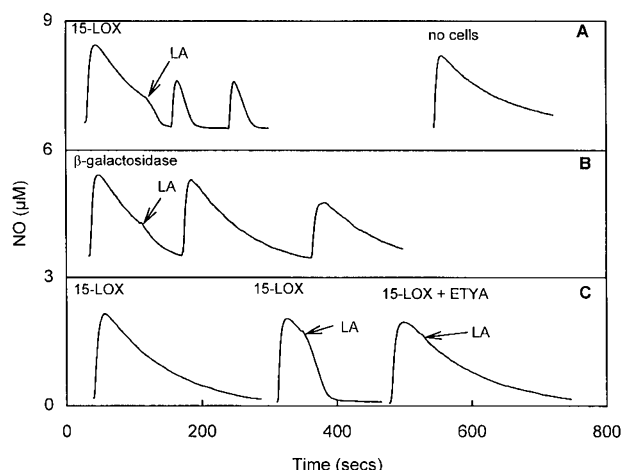


FIG. 1. Nitric oxide is consumed by 15-LOX transfectants. PA317 transfectants expressing either human 15-LOX or β -galactosidase were added to 1 ml of 0.1 M potassium phosphate (pH 7.4), 0.2% cholate, 100 μM DTPA, and monitored for rates of NO consumption at 37 °C. **Panel A**, nitric oxide consumption by 15-LOX transfectants. **Left trace**, NO (1.9 μM) was added to 15-LOX transfectants (1.7×10^6 cells) and monitored before and after addition of 500 μM linoleate (LA). Once NO was consumed, two further 1.9 μM NO additions were made. **Right trace**, decay rate of NO in the absence of cells. **Panel B**, nitric oxide consumption by β -galactosidase transfectants: NO (1.9 μM) was added to β -galactosidase transfectants (1.7×10^6 cells) and monitored before and after addition of 500 μM linoleate (LA). Once NO was consumed, two further 1.9 μM NO additions were made. **Panel C**, inhibition of cellular nitric oxide consumption by ETYA. 15-LOX transfectants (2×10^6 cells) were preincubated in 1 ml of PBS in the NO electrode for 10 min at 37 °C with/without 100 μM ETYA before addition of 1.9 μM NO and 500 μM linoleate (LA). Results shown are of a representative experiment repeated at least three times.

trated lipids, mass spectroscopic analyses were performed on an API III triple quadrupole mass spectrometer (PE-Sciex, Concord, Ontario, Canada) following reversed-phase HPLC as described previously (24, 32).

Rapid Kinetic Stopped Flow Measurements of (13S)-HPODE-induced 15-LOX Fluorescence Quenching—As an index of activation, the rate and extent of intrinsic tryptophan fluorescence quenching by (13S)-HPODE was monitored with and without NO. (13S)-HPODE stock (14 μM) was prepared in 2 ml of 0.1 M potassium phosphate buffer, pH 7.4, with 0.2% cholate and 100 μM DTPA. Soybean 15-LOX was diluted to 1.76 μM in 0.1 M potassium phosphate buffer, pH 7.4, containing 100 μM DTPA, immediately prior to use. The HPODE and 15-LOX solutions were placed in separate drive syringes for assay, and equal volumes were mixed during each measurement. Rapid kinetic stopped-flow studies were carried out on a Hi-Tech SF-53 stopped flow spectrophotometer with a dead time of 1.2 ms. Changes in fluorescence emission above 320 nm were monitored using a cut-off filter, with excitation at 280 nm. Nitric oxide was added to HPODE solution with a final concentration 5.4 μM and immediately placed into the drive syringe for assay.

RESULTS

Characterization of NO Loss in Reaction Systems—Nitric oxide (1.9 μM) decay in 1 ml of aerobic phosphate buffer followed first order kinetics with a rate constant (k_{obs}) of $4.1 \pm 0.6 \times 10^{-3}\text{ s}^{-1}$. Aerobic oxidation of NO follows second order kinetics (51), but at the low NO concentrations utilized in this study the rate of NO autooxidation is slow and alternative reactions that follow first order kinetics predominate (*e.g.* NO-electrode reaction, diffusion into gas phase). Using the calculated k_{obs} , the rate of background NO loss can therefore be calculated at any point during the time course.

Cells Transfected with Human 15-LOX Consume NO during Linoleate Oxidation—Rates of NO decay were higher than in buffer alone when added to murine fibroblast PA317 cells expressing either 15-LOX or β -galactosidase (controls) and no longer followed first order kinetics (Fig. 1A). For example, at 1 μM NO, the rate of decay is $0.25\text{ }\mu\text{M min}^{-1}$ in buffer alone, or $0.64 \pm 0.08\text{ }\mu\text{M min}^{-1}$ and $0.61 \pm 0.07\text{ }\mu\text{M min}^{-1}$ (mean \pm S.D.,

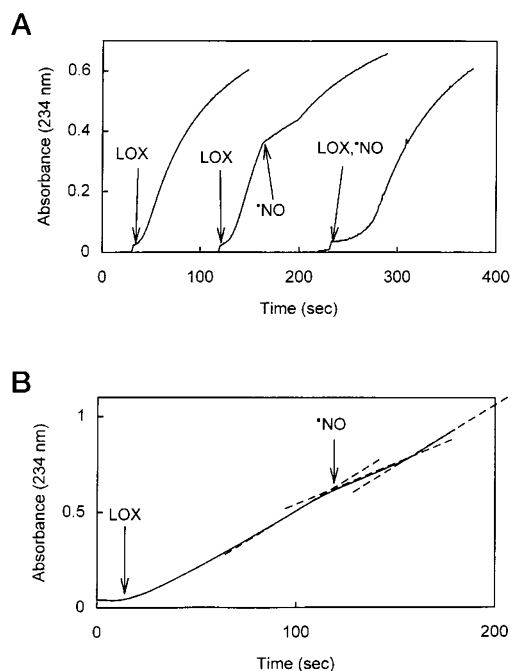


FIG. 2. **Nitric oxide reversibly inhibits 15-LOX.** Rabbit (panel A, 6.5 nM enzyme) or soybean (panel B, 0.88 nM enzyme) 15-LOX was added to 2 ml of 0.1 M potassium phosphate (pH 7.4), 0.2% cholate, 100 μ M DTPA, 500 μ M linoleate, and conjugated diene formation monitored at 235 nm. Nitric oxide (1.9 μ M) was added where indicated by arrows. Results shown are of a representative experiment repeated at least three times.

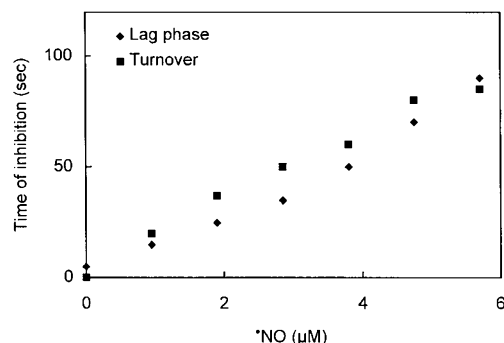


FIG. 3. **Time of inhibition of rabbit 15-LOX by nitric oxide.** Nitric oxide was added to rabbit 15-LOX oxidation assays, as described in Fig. 2, during turnover (■) or prior to 15-LOX addition (◆), and time of inhibition determined.

$n = 3$) for 1.7×10^6 15-LOX transfectants and β -galactosidase controls, respectively (Fig. 1, A and B). This indicates that cell-dependent \cdot NO consuming reactions are taking place. Addition of linoleate (200–500 μ M) induced a 4.8-fold increase in the rate of 15-LOX transfectant-dependent \cdot NO consumption ($2.9 \pm 0.2 \mu\text{M min}^{-1}$, or $1.7 \pm 0.11 \text{ nmol min}^{-1} 10^6 \text{ cells}^{-1}$, mean \pm S.D., $n = 3$) (Fig. 1, A and B) and had no effect on \cdot NO consumption by β -galactosidase transfectants. The linoleate-stimulated \cdot NO consumption was completely inhibited by pre-incubating 15-LOX transfectants with 100 μ M ETYA for 10 min at 37 $^{\circ}$ C before linoleate addition (Fig. 1C), indicating that \cdot NO uptake was occurring as a result of 15-LOX turnover. Under these conditions, there was no significant injury in the different cell treatment groups, as indicated by analysis of extents of cell lysis and quantitation of both cell and medium GSH and GSSG content (data not shown).

Nitric Oxide Reversibly Inhibits Purified Soybean and Rabbit 15-LOX—Addition of 1–6 μ M \cdot NO to rabbit 15-LOX during turnover immediately inhibited conjugated diene formation.

TABLE I

Rates of conjugated diene formation and nitric oxide consumption by 15-LOX

Diene conjugation rates were measured in 2 ml of 0.1 M potassium phosphate, 500 μ M linoleate, 0.2% cholate, and 100 μ M DTPA, pH 7.4 at 37 $^{\circ}$ C with stirring. Nitric oxide (1.9 μ M) was then added during turnover. Rates of \cdot NO consumption were measured in 1 ml of phosphate buffer, 0.2% cholate, 500 μ M linoleate, 100 μ M DTPA, pH 7.4 at 37 $^{\circ}$ C with stirring, and rates of \cdot NO disappearance monitored using an \cdot NO electrode. Results shown are mean \pm S.D., $n = 3$.

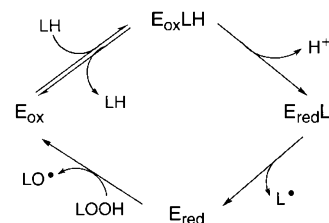
| Lipoxygenase | Conjugated diene formation | | Nitric oxide consumption |
|----------------|---|--------------|--------------------------|
| | – ·NO | + ·NO | |
| | <i>mmol min⁻¹ μmol⁻¹ 15-LOX</i> | | |
| Rabbit 15-LOX | 3.6 ± 0.15 | 0.73 ± 0.13 | 0.69 ± 0.03 |
| Soybean 15-LOX | 28.6 ± 1.0 | 18.1 ± 0.119 | 2.9 ± 0.8 |

For example, with 1.9 μ M \cdot NO, activity was inhibited 80% (Fig. 2A). If \cdot NO was added before 15-LOX, inhibition appeared as a prolongation of the lag phase (Fig. 2A). With the soybean 15-LOX, there was less inhibition than with the rabbit 15-LOX (Fig. 2B). For example, when 1.9 μ M \cdot NO was added during turnover, only 40% inhibition occurred.

For both rabbit and soybean 15-LOX, inhibition was reversible, with time of inhibition directly related to the concentration of added \cdot NO. Since soybean 15-LOX does not self-inactivate, full recovery of activity was observed following the inhibition phase. Plotting the time of inhibition versus \cdot NO concentration for the rabbit 15-LOX yielded a linear relationship with similar slopes, independent of whether \cdot NO was added to samples before 15-LOX ($m = 14.7 \text{ s } \mu\text{M}^{-1}$, $r = 0.97$), or after, during dioxygenase turnover ($m = 14.9 \text{ s } \mu\text{M}^{-1}$, $r = 0.98$) (Fig. 3).

Nitric Oxide Is Consumed during 15-LOX Turnover—Rates of \cdot NO consumption by both the rabbit and soybean 15-LOXs were examined in the presence of linoleate (Table I, Fig. 4). No uptake of \cdot NO occurred in the absence of linoleate, or if linoleate was replaced with the 15-LOX product (13S)-HPODE (Fig. 4, A and B). Addition of 750 units/ml CuZn superoxide dismutase to 15-LOX plus linoleate did not affect rates of \cdot NO consumption, indicating that superoxide ($\text{O}_2^{\cdot-}$) was not the species reacting with \cdot NO (data not shown). The rates of \cdot NO consumption directly paralleled inhibition of 15-LOX activity. The apparent K_m for \cdot NO consumption was $1.7 \pm 0.48 \mu\text{M}$ for the soybean 15-LOX (Fig. 4C). Since 15-LOX concentrations are 10^2 to 10^3 times lower than \cdot NO (13 nM rabbit 15-LOX, 3.5 nM soybean 15-LOX, 1.9 μ M \cdot NO), it is concluded that \cdot NO consumption is a catalytic process requiring dioxygenase turnover.

Effect of \cdot NO on Anaerobic Peroxidase Activity—To probe the mechanism of 15-LOX inhibition and \cdot NO uptake, effects of \cdot NO on anaerobic peroxidase activity were examined (Scheme 2). Since soybean 15-LOX does not self-inactivate, anaerobic peroxidase can be measured by allowing the enzyme to oxidize



SCHEME 2. Anaerobic peroxidase activity of 15-LOX. Linoleate (LH) is first oxidized to an alkyl radical by the ferric enzyme (E_{ox}), forming reduced enzyme with bound alkyl radical ($E_{\text{red}}L^{\cdot}$). In the absence of O_2 , the lipid radical dissociates from the active site, leaving reduced enzyme (E_{red}). To complete the cycle, peroxide product (LOOH) is reduced by a peroxidase activity of the enzyme, forming an alkoxyl radical, LO^{\cdot} , that dissociates to regenerate active enzyme (E_{ox}).

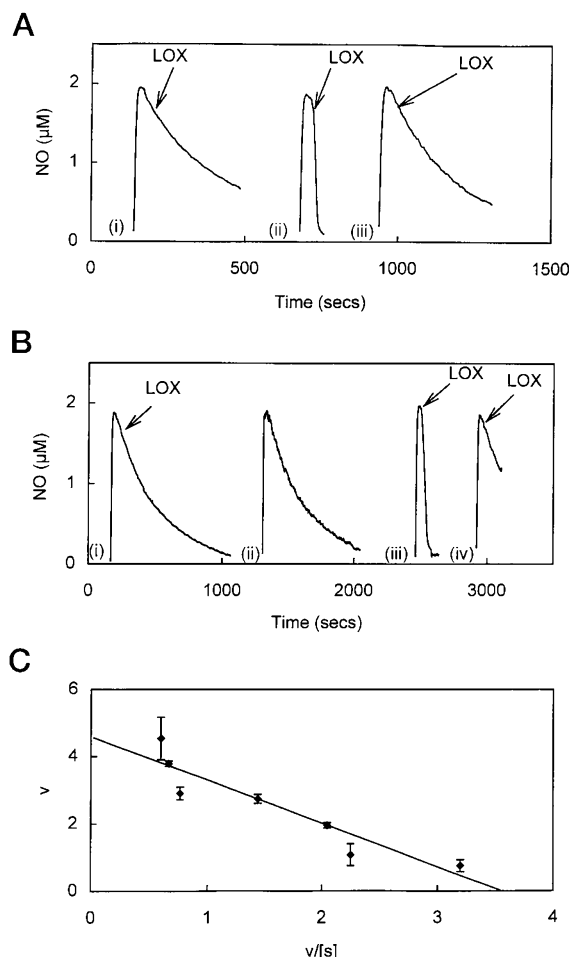


FIG. 4. Nitric oxide is consumed by lipoxygenase during dioxygenase turnover. Nitric oxide ($1.9 \mu\text{M}$) was added to 1 ml of phosphate buffer, 0.2% cholate, $100 \mu\text{M}$ DTPA, pH 7.4 at 37°C with stirring, and rates of NO disappearance monitored using an NO electrode. Arrow shows point of 15-LOX addition. *Panel A*, nitric oxide uptake by rabbit 15-LOX: (i), rabbit 15-LOX (13 nM) in buffer; (ii), rabbit 15-LOX (13 nM) plus $500 \mu\text{M}$ linoleate; (iii), rabbit 15-LOX (13 nM) plus $500 \mu\text{M}$ (13S)-HPODE. Results shown are of a representative experiment repeated at least three times. *Panel B*, nitric oxide uptake by soybean 15-LOX: (i), soybean 15-LOX (3.5 nM) in buffer; (ii), $1.9 \mu\text{M}$ NO plus $500 \mu\text{M}$ linoleate; (iii), soybean 15-LOX (3.5 nM) plus $500 \mu\text{M}$ linoleate; (iv), soybean 15-LOX (3.5 nM) plus $500 \mu\text{M}$ (13S)-HPODE. Results shown are of a representative experiment repeated at least three times. *Panel C*, determination of apparent K_m for nitric oxide consumption by soybean 15-LOX. Rates of NO consumption by 1.76 nM soybean 15-LOX were determined at varying NO concentrations and plotted as v versus $v/[s]$, where v is $\mu\text{M}/\text{min}$ and s is μM , with $n = 3$ for each NO concentration. Michaelis-Menten parameters were calculated using Enzfitter (Elsevier Biosoft).

linoleic acid until all O_2 is consumed. At this point, peroxidase activity initiates and can be monitored by measuring oxodiene formation. Sequential additions of $1.9 \mu\text{M}$ NO had no effect on anaerobic peroxidase activity, with base-line irregularities at the point of NO addition being due to opening/closing the sample chamber (Fig. 5).

Effect of NO (13S)-HPODE-induced Fluorescence Quenching—Fluorescence quenching of intrinsic tryptophan fluorescence by (13S)-HPODE is associated with 15-LOX activation and conversion from ferrous to ferric oxidation state (47, 52). Rapid kinetic stopped flow fluorescence studies were carried out using soybean 15-LOX, since large amounts of enzyme were required. No effect of NO on the rate or extent of (13S)-HPODE fluorescence quenching was observed (Fig. 6).

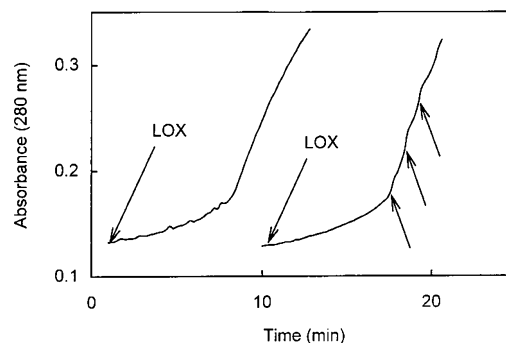


FIG. 5. Effect of nitric oxide on anaerobic peroxidase activity of soybean 15-lipoxygenase. Soybean 15-LOX (1.76 nM) was added to 2 ml of 0.1 M potassium phosphate (pH 7.4), $500 \mu\text{M}$ linoleate, 0.2% cholate, $100 \mu\text{M}$ DTPA, and formation of oxodiene products of peroxidase activity was monitored at 280 nm . Once the reaction had become fully anaerobic through LOX-mediated oxygen consumption, and peroxidase activity initiated (indicated by the increase in rate of absorbance change), aliquots of $1.9 \mu\text{M}$ NO were added (as indicated by the arrows) and rates monitored. Results shown are of a representative experiment repeated at least three times.

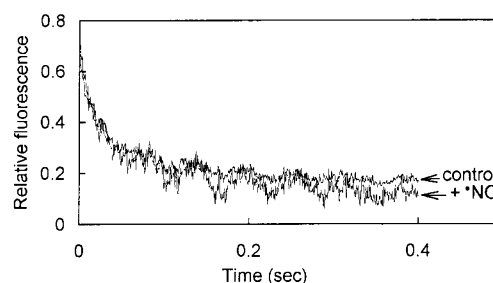


FIG. 6. Nitric oxide does not alter rate or extent of (13S)-HPODE-induced fluorescence quenching. (13S)-HPODE stock ($14 \mu\text{M}$) was prepared in 2 ml of 0.1 M potassium phosphate buffer, pH 7.4, with 0.2% cholate and $100 \mu\text{M}$ DTPA. Soybean 15-LOX was diluted to $1.76 \mu\text{M}$ in 0.1 M potassium phosphate buffer, pH 7.4 containing $100 \mu\text{M}$ DTPA, immediately prior to use. The HPODE and 15-LOX solutions were placed in separate drive syringes for assay, and equal volumes were mixed during each measurement. Where utilized, NO ($5.4 \mu\text{M}$) was added to the HPODE solution and immediately mixed with 15-LOX. Changes in fluorescence were monitored above 320 nm using a cut-off filter, with excitation at 280 nm . Traces shown are the average of several independent experiments ($n = 3$ for controls, $n = 7$ for NO samples).

Nitric Oxide Consumption during 15-Lipoxygenase Activation—High concentrations of native rabbit or soybean LOX did not consume NO in the absence of substrate (Fig. 7, A and B). Addition of equivalent amounts of bovine serum albumin shows that the small decrease in NO concentration on addition of 15-LOX alone was due to dilution or nonspecific effects of adding protein (Fig. 7A). However, addition of (13S)-HPODE to 15-LOX-containing samples resulted in NO consumption (Fig. 7, A and B). Plotting NO uptake versus enzyme concentration demonstrated a linear relationship ($m = 0.51 \pm 0.03$, $r = 0.99$), with the amount of NO consumed being approximately 2 molar eq/mol of 15-LOX (Fig. 7C). HPLC analysis showed that, during activation of 15-LOX by HPODE, NO did not induce HPODE loss (data not shown).

To examine if NO activates 15-LOX, the characteristic lag phase of 15-LOX dioxygenase activity was examined following preincubation with NO. Soybean 15-LOX (4 nM) was incubated for 15 min at 25°C with $3.8 \mu\text{M}$ NO before addition of linoleate. By the end, 95% of the added NO would have been oxidized to NO_2^- , ensuring that residual NO was insufficient to inhibit dioxygenase activity. This preincubation with NO had no effect on the time of the lag (data not shown), indicating that NO was not activating 15-LOX.

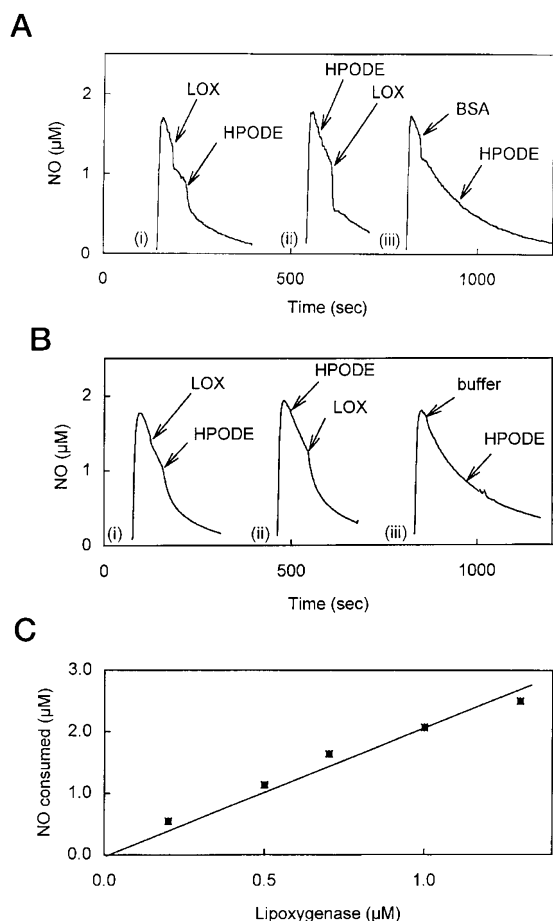


FIG. 7. Nitric oxide is consumed during activation of 15-LOX by (13S)-HPODE. Panel A, consumption of nitric oxide by rabbit 15-LOX during (13S)-HPODE activation. Nitric oxide ($1.9 \mu\text{M}$) was added to 1 ml 0.1 M potassium phosphate buffer, pH 7.4, with 0.2% cholate and $100 \mu\text{M}$ DTPA at 37°C , and rates of NO disappearance monitored using an NO electrode. (i), rabbit 15-LOX ($0.113 \mu\text{M}$) was added, then $2 \mu\text{M}$ (13S)-HPODE; (ii), $2 \mu\text{M}$ (13S)-HPODE was added, then rabbit 15-LOX ($0.113 \mu\text{M}$); (iii), bovine serum albumin (protein concentration and volume equivalent to added 15-LOX) was added, then $2 \mu\text{M}$ (13S)-HPODE. Results shown are of a representative experiment repeated at least three times. Panel B, uptake of nitric oxide by soybean 15-LOX during (13S)-HPODE activation. Nitric oxide ($1.9 \mu\text{M}$) was added to 1 ml of 0.1 M potassium phosphate buffer, pH 7.4, with 0.2% cholate and $100 \mu\text{M}$ DTPA, and rates of NO disappearance monitored. (i), soybean 15-LOX ($0.22 \mu\text{M}$) was added, then $2 \mu\text{M}$ (13S)-HPODE; (ii), $2 \mu\text{M}$ (13S)-HPODE was added, then soybean 15-LOX ($0.22 \mu\text{M}$); (iii), 0.1 M potassium phosphate buffer (volume equivalent to 15-LOX) was added, then $2 \mu\text{M}$ (13S)-HPODE. Results shown are of a representative experiment repeated at least three times. Panel C, ratio of nitric oxide consumption/mol of soybean LOX during (13S)-HPODE activation. Total amounts of NO consumed during soybean 15-LOX activation were measured as in panel B and plotted against 15-LOX concentration.

Fate of Linoleic Acid Oxidized by 15-LOX in the Presence of NO —To determine the fate of linoleate oxidized by 15-LOX in the presence of NO , lipid products were analyzed by HPLC. Using soybean 15-LOX, a fixed amount of substrate could be completely oxidized ($100 \mu\text{M}$) in the presence or absence of NO and the yield of products compared. Due to concurrent 15-LOX inhibition by NO , the times for complete linoleate oxidation approximately doubled. For organic solvent extraction of free linoleate and its oxidation products, acidic conditions maximized yield. However, small amounts of NO_2^- , present as a decomposition product of NO , will nitrate lipid hydroperoxides at low pH, thus depleting LOOH and yielding L(O)NO_2 (53). To avoid this artifact during extraction of 15-LOX products, con-

taminating NO_2^- was first removed by reaction with sulfanilamide/HCl and *N*-(1-naphthyl)ethylenediamine. Control experiments determined that this completely protects LOOH from nitration by acidified NO_2^- (data not shown). By both reverse phase HPLC and quantitation of total hydroperoxide yields, the predominant product was HPODE (Fig. 8, A and B). No difference in HPODE yield occurred if NO was present during dioxygenase turnover. Analysis by normal phase and chiral phase HPLC showed that the HPODE was predominantly the (13S) isomer (Fig. 8C). Electrospray mass spectrometry revealed no nitrogen-containing oxidized lipid species (data not shown), indicating that the product profile of 15-LOX is unchanged by NO .

The Influence of 15-LOX Catalytic Activity on NO -dependent Activation of Soluble Guanylate Cyclase—Addition of the NO donor DEA-NONOate, in a concentration that yielded $\sim 400 \text{ nM}$ NO in the absence of 15-LOX-mediated peroxy radical formation, activated soluble guanylate cyclase formation of cGMP from GTP. Addition of 15-LOX alone had no effect on extents of cGMP formation unless substrate ($5 \mu\text{M}$ arachidonate) was added, whereupon there was an extensive and significant 82% decrease in soluble guanylate cyclase activity and cGMP formation (Fig. 9). Since fatty acids may inhibit soluble guanylate cyclase, control experiments were performed to reveal effects of native and oxidized arachidonate on extents of cGMP formation. 15-Lipoxygenase oxidation of $5 \mu\text{M}$ arachidonate was allowed to go to completion, prior to addition to reaction systems containing soluble guanylate cyclase, [$\alpha\text{-}^{32}\text{P}$]GTP, and DEA-NONOate. Soluble guanylate cyclase was not significantly inhibited by either native or oxidized arachidonate (data not shown). This affirmed that NO reaction with and consumption by enzyme-bound peroxy radical intermediates during catalytic cycling of 15-LOX turnover was responsible for inhibition of guanylate cyclase, rather than direct guanylate cyclase inactivation by oxidized lipid products that are formed during 15-LOX oxidation of arachidonate.

DISCUSSION

These results show that the vascular signal transduction actions of both NO and lipoxygenase products can be interdependent, since NO inhibits rates of 15-LOX product formation and, in turn, 15-LOX catalytic activity consumes NO and thus impairs guanylate cyclase activation. These findings may in part explain the anti-atherogenic and anti-cell proliferative actions of NO that have been observed in animal models following L-arginine feeding, administration of NO synthase inhibitors, or transfection with nitric-oxide synthase (54–57). The experiments reported herein were designed to model mechanisms of NO interactions with lipoxygenase-mediated lipid oxidation and to reflect conditions that exist in the vascular compartment. For example, the expression of 15-LOX by cells stably transfected with the human 15-LOX gene is approximately the same as mouse peritoneal macrophages (44); thus, the observed cell 15-LOX-dependent rates of NO consumption are well within those to be expected physiologically ($\sim 0.85 \text{ nmol min}^{-1} 10^6 \text{ cells}^{-1}$; Fig. 1). Maximal rates of $\text{NO}_2^-/\text{NO}_3^-$ production in activated rat peritoneal macrophages or murine RAW264.7 macrophages are 0.1 and 0.2 $\text{nmol min}^{-1} 10^6 \text{ cells}^{-1}$, respectively (58, 59), much lower than the rates of NO consumption observed here. Therefore, it would be expected that the range of 15-LOX expression in normal and diseased vasculature would have a significant effect on NO available for soluble guanylyl cyclase activation and cell-mediated host defenses. This was confirmed by the observation that NO -activated soluble guanylate cyclase formation of cGMP was profoundly suppressed during the catalytic oxidation of arachidonate by 15-LOX.

FIG. 8. Analysis of lipid product profile following nitric oxide consumption by soybean 15-LOX. Panel A, samples prepared as described under "Experimental Procedures" were analyzed for total LOOH by horseradish peroxidase-catalyzed oxidation of leukomethylene blue ($n = 4$, \pm S.D.) Panel B, following extraction into organic solvent, samples were analyzed for total HPODE content using reverse phase HPLC. Panel C, to examine isomer content of samples prepared in the presence of $\cdot\text{NO}$, samples were also analyzed by normal phase (panel C) and chiral phase (inset) HPLC.

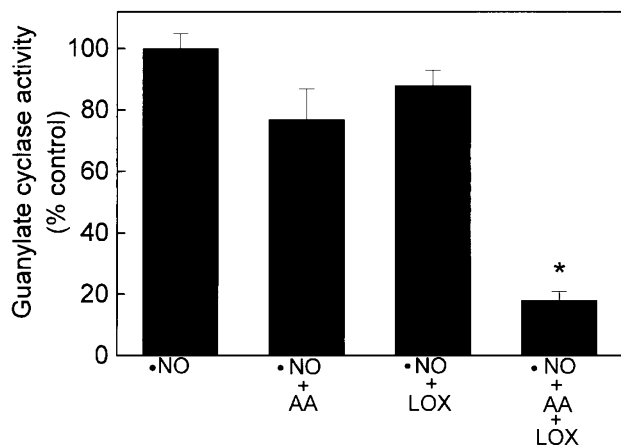
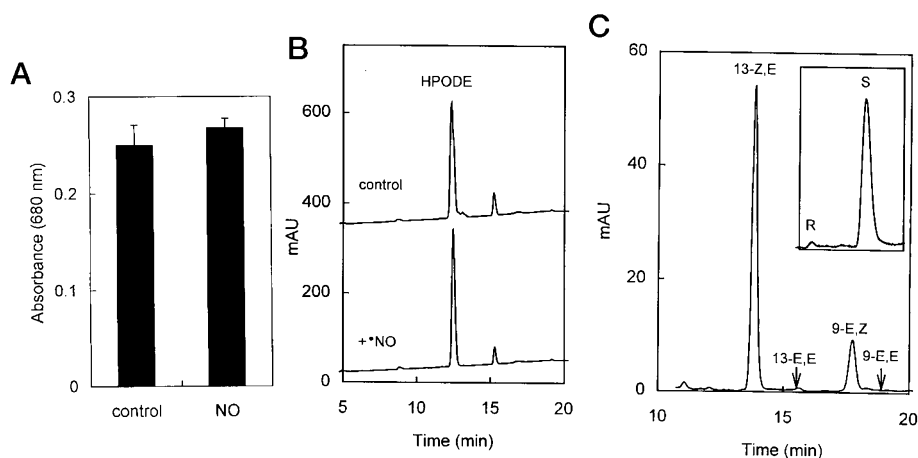


FIG. 9. 15-Lipoxygenase-mediated arachidonate oxidation impairs nitric oxide-dependent signaling by inhibiting soluble guanylate cyclase activation. Nitric oxide activation of soluble guanylate cyclase was determined in the presence of 1.3 nM rabbit 15-LOX plus 0 or 5 μM arachidonate. Experiments were replicated at least three times with similar results, with reported determinations having $n = 3$. * represents $p < 0.05$ following analysis of variance and Bonferroni/Dunn *post hoc* test analysis.

To define the mechanism(s) of $\cdot\text{NO}$ reaction with and consumption by 15-LOX, studies were carried out using purified rabbit reticulocyte and soybean 15-LOX. For both enzymes, reversible inhibition was observed on addition of 1–6 μM $\cdot\text{NO}$ (Fig. 2). Inhibition coincided with $\cdot\text{NO}$ consumption, and activity was recovered once $\cdot\text{NO}$ was depleted. For $\cdot\text{NO}$ consumption, addition of linoleate but not (13S)-HPODE was required (Fig. 4) and $\cdot\text{NO}$ consumption was catalytic. These data suggest that an intermediate or product of the dioxygenase cycle react with $\cdot\text{NO}$ to inhibit 15-LOX.

The 15-LOX intermediates that may react with $\cdot\text{NO}$ are shown in Scheme 1. Since linoleate was required (Fig. 4), the oxidized enzyme (E_{ox}), containing Fe^{3+} , is unlikely to be the site of $\cdot\text{NO}$ consumption. Another possible reaction site is $\text{E}_{\text{red}}\text{L}$. However, since $\cdot\text{NO}$ had no effect on anaerobic peroxidase activity (Fig. 5), a role for this species in $\cdot\text{NO}$ consumption is unlikely. In addition, the low concentrations of $\cdot\text{NO}$ used in these experiments are unlikely to compete efficiently with O_2 , initially present at 240 μM , for reaction with L bound at the active site. Finally, the observation that (13S)-HPODE was the major product indicated that $\cdot\text{NO}$ addition occurs after stereospecific O_2 insertion has taken place.

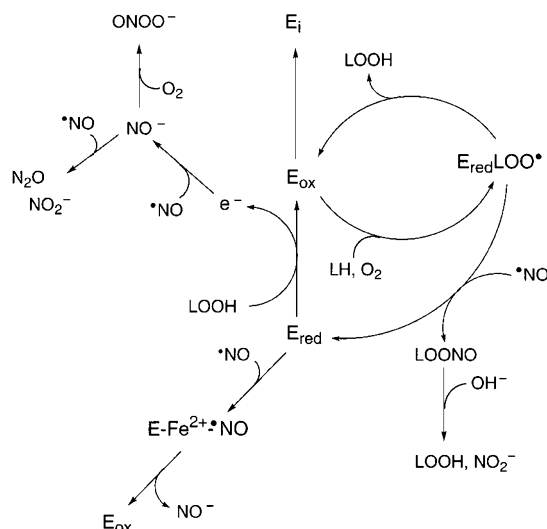
Native 15-LOX contains reduced iron and is inactive until oxidized by the product, (13S)-HPODE. During dioxygenase turnover, this results in a characteristic lag phase that can be abolished by prior addition of a small amount of product. At

high concentrations of $\cdot\text{NO}$, a nitrosyl complex forms with the reduced ferrous iron of 15-LOX (29–31). It is therefore possible that $\cdot\text{NO}$ could compete with (13S)-HPODE for reaction with reduced 15-LOX iron. However, using stopped flow fluorescence, no effect of $\cdot\text{NO}$ on either the rate or extent of 15-LOX intrinsic tryptophan fluorescence quenching was found (Fig. 6) (47, 52). Additionally, native 15-LOX did not consume $\cdot\text{NO}$ (Fig. 7) and the time of $\cdot\text{NO}$ inhibition was independent of (13S)-HPODE concentration (Fig. 3). It was recently shown and confirmed herein, that $\cdot\text{NO}$ prolongs the lag phase of 15-LOX activity (Fig. 4, Ref. 25). Inhibition of 15-LOX did not require addition of $\cdot\text{NO}$ before substrate, since the length of $\cdot\text{NO}$ inhibition is the same, whether $\cdot\text{NO}$ was added either before or during enzyme turnover (Fig. 3). This shows that $\cdot\text{NO}$ is not preventing 15-LOX activation and infers that enzyme inhibition results from reaction with a dioxygenase intermediate.

15-LOX did not consume $\cdot\text{NO}$ in the absence of (13S)-HPODE, thus nitrosyl complexes with reduced 15-LOX metal centers did not form. This is not unexpected, since previous studies determined a dissociation constant ($K_d = 95 \mu\text{M}$ at pH 7.0) for the major EPR species formed between $\cdot\text{NO}$ and soybean 15-LOX, far in excess of $\cdot\text{NO}$ concentrations used in this study and those found biologically. A second species was also observed by EPR previous study of $\cdot\text{NO}$ -15-LOX reactions (31). Since formation of this signal required at least 400 μM $\cdot\text{NO}$, it is also a biologically unlikely explanation of 15-LOX inhibition by $\cdot\text{NO}$.

Two previous reports suggested that high concentrations of $\cdot\text{NO}$ could oxidize native 15-LOX, leading to either activation or formation of a species more susceptible to peroxide activation (25, 29). In both studies, electron transfer may have occurred following formation of the iron nitrosyl complex, since it was detectable by EPR spectroscopy. Herein, low concentrations of $\cdot\text{NO}$ did not activate 15-LOX. The high K_d for formation of the EPR-detectable $\text{Fe}^{2+}\text{-NO}$ species infers that under physiological conditions, where $\cdot\text{NO}$ concentrations will be less than 1 μM , both the formation of ferrous-nitrosyl complexes and activation of 15-LOX by $\cdot\text{NO}$ is unlikely. During activation by HPODE, consumption of 2 mol of $\cdot\text{NO}$ /mol of 15-LOX was observed. Reduction of $\cdot\text{NO}$ to NO^- by the ferrous iron-derived electron, followed by secondary reactions of NO^- that can consume $\cdot\text{NO}$ (e.g. $\text{HNO} + 2\text{NO} \rightarrow \text{N}_2\text{O} + \text{NO}_2^-$, $k = 10^9 \text{ M}^{-1} \text{ s}^{-1}$) may explain these observations.

Since $\cdot\text{NO}$ had no effect on 15-LOX tryptophan fluorescence quenching, $\cdot\text{NO}$ uptake during activation is also unlikely to cause enzyme inhibition (Fig. 6). Therefore, $\cdot\text{NO}$ must react at an additional site during dioxygenase turnover. The only intermediate that was not excluded experimentally or theoretically is $\text{E}_{\text{red}}\text{LOO}$. Reaction of $\cdot\text{NO}$ with free LOO in aqueous solu-



SCHEME 3. Potential sites of nitric oxide reaction during 15-LOX oxidation of lipid. Three sites of potential NO reaction are shown. (i) During peroxide (LOOH) activation of LOX, 2 mol of NO are consumed, via reaction with an electron (e^-) released from the ferrous enzyme (E_{red}) to form nitroxyl anion (NO^-). Secondary reactions of NO^- will consume further NO molecules, for example, reaction of NO^- with O_2 or with further NO molecules, as shown. (ii) During dioxygenase turnover, NO is consumed through reaction with $E_{\text{red}}\text{LOO}^*$ to form reduced inactive enzyme (E_{red}) and an organic peroxynitrite (LOONO). This hydrolyzes to the hydroperoxide (LOOH) and nitrite (NO_2^-). (iii) At higher NO concentrations a ferrous nitrosyl complex can form ($E\text{-Fe}^{2+}\text{-NO}$), which slowly decomposes, yielding active enzyme (E^*).

tion is extremely fast ($k = 1\text{--}2 \times 10^9 \text{ M}^{-1} \text{ s}^{-1}$; Refs. 15, 19, and 31). Since NO can diffuse into the active site of LOX, as well as concentrate in lipophilic milieu, a reaction of NO with $E_{\text{red}}\text{LOO}^*$ is highly plausible.

If NO reacts with $E_{\text{red}}\text{LOO}^*$ to form LOONO , dissociation of this product from the active site would leave reduced enzyme (E_{red}) that requires reactivation by HPODE for completion of the catalytic cycle (Scheme 3). Activation of soybean 15-LOX is approximately 20% of the rate of linoleate dioxygenation (60), while activation of rabbit 15-LOX is 10% of the rate-limiting step of dioxygenase activity (0.59 s^{-1} versus 6.4 s^{-1} , Ref. 61). Therefore, promoting formation of the inactive enzyme E_{red} by NO reaction with $E_{\text{red}}\text{LOO}^*$ will significantly decrease the overall rate of dioxygenase activity and product yield (Scheme 3).

The product of reaction between NO and LOO^* , an organic peroxynitrite (LOONO), has at least two possible fates in aqueous conditions. First, it can hydrolyze, forming LOOH and NO_2^- . Second, it can decompose ($t_{1/2} = 0.2\text{--}0.6 \text{ s}$, Ref. 36) to form the caged radicals, $[\text{LO}^* \text{NO}_2]$. These either recombine to form LONO_2 , an alkyl nitrate, or dissociate to free species, which can react with additional molecules of NO , forming LONO and NO_2^- , respectively. The relative contribution of each of these pathways to LOONO decomposition is unknown. Since identical amounts of HPODE were formed either in the presence or absence of NO and no LNO_2 , LONO_2 , or LONO was found, hydrolysis of LOONO generated at the 15-LOX active site to LOOH and NO_2^- is likely.

A previous report showed that NO reaction with soybean 15-LOX during oxidation of 1-palmitoyl-2-arachidonoyl-*sn*-glycero-3-phosphocholine liposomes as substrate formed LONO_2 , LNO_2 , $\text{LOOH}(\text{NO}_2)$, and $\text{LOH}(\text{NO}_2)$ (32). Herein, experiments have been designed to ensure that (i) all added NO is consumed through direct reaction with 15-LOX intermediates and (ii) enzyme turnover did not significantly deplete oxygen, thus avoiding LOOH decomposition and formation of secondary radicals such as LO^* and L^* that can react rapidly with NO and

NO_2 to form nitrated products (35, 62, 63). Finally, treatment of samples with 1% sulfanilamide, 3 N HCl and 0.02% *N*-(1-naphthyl)-ethylenediamine before extraction ensured removal of NO_2^- , which at low pH will nitrosate LOOH to form nitrated lipids (53).

In summary, our data show that at NO and 15-LOX concentrations found in tissues, (a) 15-LOX is inhibited, (b) 15-LOX catalytic activity impairs NO -dependent activation of soluble guanylate cyclase, and (c) 15-LOX consumes NO through two separate mechanisms. First, during peroxide-mediated activation of 15-LOX, 2 mol of NO /mol of 15-LOX are consumed. Second, reaction of NO with an intermediate of the dioxygenase cycle, $E_{\text{red}}\text{LOO}^*$, leads to reversible enzyme inhibition by promoting formation of the inactive ferrous enzyme, E_{red} . While NO reaction during 15-LOX catalysis leads to no change in product profile, significant suppression of HPODE generation occurred in concert with consumption of significant quantities of NO .

Since modulation of 15-LOX activity by NO occurs at biologically relevant NO concentrations, suppression of HPODE formation and NO consumption is expected *in vivo*. The K_d for NO activation of soluble guanylyl cyclase is approximately 250 nM (64); therefore, varying NO levels around these concentrations will have significant impact on cGMP production and resultant smooth muscle relaxation, as revealed in Fig. 9. Thus, consumption of NO by the elevated lipoxygenase activities present in a variety of hypertensive vascular diseases would then contribute to their characteristic reduced responses to NO (40–42).

REFERENCES

1. Yamamoto, S., and Smith, W. L. (1995) *J. Lipid Med. Cell Signal* **12**, 195.
2. Hamberg, M., and Samuelsson, B. (1974) *Proc. N. Y. Acad. Sci. U. S. A.* **71**, 3400–3404.
3. Yokoyama, C., Shinjo, F., Yoshimoto, T., Yamamoto S., Oates, J. A., and Brash, A. R. (1986) *J. Biol. Chem.* **261**, 16714–16721.
4. Kühn, H. (1996) *Prog. Lipid Res.* **35**, 203–226.
5. Rapoport, S. M., Schewe, T., and Thiele, B. J. (1990) in *Blood Cell Biochemistry* (Harris, J. R., ed) Vol. 1, p. 151, Plenum, New York.
6. Kühn, H., Belkner, J., Zaiss, S., Fahrenklemper, T., and Wohlfeil, S. (1994) *J. Exp. Med.* **179**, 1903–1911.
7. Ylä-Herttuala, S., Rosenfeld, M. E., Parthasarathy, S., Glass, C. K., Sigal, E., Sarkioia, T., Witztum, J. T., and Steinberg, D. (1991) *J. Clin. Invest.* **87**, 1146–1152.
8. Folcik, V. A., Nivar-Aristy, R. A., Krajewski, L. P., and Cathcart, M. K. (1995) *J. Clin. Invest.* **96**, 504–510.
9. Belkner, J., Stender, H., and Kühn, H. (1998) *J. Biol. Chem.* **273**, 23225–23232.
10. Parthasarathy, S., Wieland, E., and Steinberg, D. (1989) *Proc. Natl. Acad. Sci. U. S. A.* **86**, 1046–1050.
11. Rankin, S. M., Parthasarathy, S., and Steinberg, D. (1991) *J. Lipid Res.* **32**, 449–456.
12. O'Leary, V. J., Graham, A., Stone, D., and Darley-Usmar, V. M. (1996) *Free Radical Biol. Med.* **20**, 525–532.
13. Ylä-Herttuala, S., Luoma, J., Viita, H., Hiltunen, T., and Nikkari, T. (1995) *J. Clin. Invest.* **95**, 2692–2698.
14. Harata, D., Kurihara, H., Levkovitz, H., Shaish, A., and Sigal, E. (1997) *Atherosclerosis* **134**, 279 (abstr.).
15. Shen, J., Herderick, E., Cornhill, J. F., Zsigmond, E., Kim, H. S., Kühn, H., Guevara, N. V., and Chan, L. (1998) *J. Clin. Invest.* **98**, 2201–2208.
16. Sendobry, S. M., Cornicelli, J. A., Welch, K., Tait, B., Trivedi, B. K., Colby, N., Dyer, R. D., Feinmark, S. J., and Daugherty, A. (1997) *Br. J. Pharmacol.* **120**, 1199–1206.
17. Malo-Ranta, U., Ylä-Herttuala, Metsä-Ketelä, T., Jaakkola, O., Moilanen, E., Vourinen, P. and Nikkari, T. (1994) *FEBS Lett.* **337**, 179–183.
18. O'Donnell, V. B., Chumley, P. H., Hogg, N., Bloodsworth, A., Darley-Usmar, V. M., and Freeman, B. A. (1997) *Biochemistry* **36**, 15216–15223.
19. Hayashi, K., Noguchi, N., and Niki, E. (1995) *FEBS Lett.* **370**, 37–40.
20. Goss, S. P. A., Hogg, N., and Kalyanaraman, B. (1995) *Chem. Res. Toxicol.* **8**, 800–806.
21. Jessup, W., Mohr, D., Gieseg, S. P., Dean, R. T., and Stocker, R. (1992) *Biochim. Biophys. Acta* **1180**, 73–82.
22. Hogg, N., Kalyanaraman, B., Joseph, J., Struck, A., and Parthasarathy, S. (1993) *FEBS Lett.* **334**, 170–174.
23. Yates, M. T., Lambert, L. E., Whitten, J. P., McDonald, I., Mano, M., Ku, G., and Mao, S. J. T. (1992) *FEBS Lett.* **309**, 135–138.
24. Rubbo, H., Radi, R., Trujillo, M., Telleri, R., Kalyanaraman, B., Barnes, S., Kirk, M. and Freeman, B. A. (1994) *J. Biol. Chem.* **269**, 26066–26075.
25. Weisner, R., Rathmann, J., Holzthütter, H. G., Stöer, R., Mäder, K., Nolting, H., and Kühn, H. (1996) *FEBS Lett.* **389**, 229–232.
26. Holzthütter, H. G., Wiesner, R., Rathmann, J., Stöer, R., and Kühn, H. (1997) *Eur. J. Biochem.* **245**, 608–616.

27. Kanner, J., Harel, S., and Granit, R. (1992) *Lipids* **27**, 46–49
28. Kuban, R. J., Weisner, R., Rathman, J., Veldink, G., Nolting, H., Sole, V. A., and Kühn, H. (1998) *Biochem. J.* **332**, 237–242
29. Galpin, J. R., Veldink, G. A., Vliegthart, J. F. G., and Boldingh, J. (1978) *Biochim. Biophys. Acta* **536**, 356–362
30. Salerno, J. C., and Siedow, J. N. (1979) *Biochim. Biophys. Acta* **579**, 246–251
31. Nelson, M. J. (1987) *J. Biol. Chem.* **262**, 12137–12142
32. Rubbo, H., Parthasarathy, S., Barnes, S., Kirk, M., Kalyanaraman, B., and Freeman, B. A. (1995) *Arch. Biochem. Biophys.* **324**, 15–25
33. Liu, X., Miller, M. J. S., Joshi, M. S., Thomas, D. D., and Lancaster, J. R. (1998) *Proc. Natl. Acad. Sci. U. S. A.* **95**, 2175–2179
34. Brovkovich, V., Stolarczyk, E., Oman, J., Tomboulia, P., and Malinski, T. (1999) *J. Pharm. Biomed. Anal.* **19**, 135–143
35. Wallington, T. J., Dagaut, P., and Kurylo, M. J. (1992) *Chem. Rev.* **92**, 667–710
36. Padmaja, S., and Huie, R. E. (1993) *Biochem. Biophys. Res. Commun.* **195**, 539–544
37. Liu, X., Miller, M. J. S., Joshi, M. S., Sadowska-Krowicka, H., Clark, D. A., and Lancaster, J. R., Jr. (1998) *J. Biol. Chem.* **273**, 18709–18713
38. Ignarro, L. J., Buga, G. M., Byrns, R. E., Wood, K. S., and Chaudhri, G. (1988) *J. Pharmacol. Exp. Ther.* **246**, 218–226
39. Gryglewski, R. J., Palmer, R. M., and Moncada, S. (1986) *Nature* **320**, 454–456
40. Verbeuren, T. J., Jordaens, F. H., Van Hove, C. E., Van Hoydonck, A. E., and Herman, A. G. (1990) *Eur. J. Pharmacol.* **191**, 173–184
41. Minor, R. L., Myers, P. R., Guerra, R., Bates, J. N., and Harrison, D. G. (1990) *J. Clin. Invest.* **86**, 2109–2116
42. White, C. R., Darley-Usmar, V., McAdams, M., Berrington, W. R., Gore, J., Thompson, J. A., Parks, D. A., Tarpey, M. M., and Freeman, B. A. (1996) *Proc. Natl. Acad. Sci. U. S. A.* **93**, 8745–8749
43. Belkner, J., Wiesner, R., Rathmann, J., Barnett, J., Sigal, E., and Kühn, H. (1993) *Eur. J. Biochem.* **213**, 251–261
44. Benz, D. J., Mol, M., Ezaki, M., Mori-Ito, N., Zelán, I., Miyanohara, A., Friedmann, T., Parthasarathy, S., Steinberg, D., and Witztum, J. L. (1996) *J. Biol. Chem.* **270**, 5191–5197
45. Miyanohara, A., Sharkey, M. F., Witztum, J. L., Steinberg, S., and Friedmann, T. (1988) *Proc. Natl. Acad. Sci. U. S. A.* **85**, 6538–6542
46. Hamberg, M., and Samuelsson, B. (1967) *J. Biol. Chem.* **242**, 5329–5335
47. Egmond, M. R., Finazzi-Agrò, A., Fasella, P. M., Veldink, G. A., and Vliegthart, J. F. G. (1975) *Biochim. Biophys. Acta* **375**, 43–49
48. Schewe, T., Kühn, H., and Rapoport, S. M. (1987) in *Prostaglandins and Related Substances: A Practical Approach* (Benedetto, C., McDonald-Gibson, R. G., Nigam, S., and Slater, T. F., eds) pp. 229–242, IRL Press, Oxford
49. Schultz, G., and Boehme, E. (1984) in *Methods of Enzymatic Analysis* Bergmeyer, H. U., Bergmeyer, J., and Grassl, M., eds) pp. 379–389, Verlag Chemie, Weinheim, Germany
50. Auerbach, B. J., Kiely, J. S., and Cornicelli, J. A. (1992) *Anal. Biochem.* **201**, 375–380
51. Ignarro, L. J., Fukito, J. M., Griscavage, J. M., Rogers, N. E., and Burns, R. E. (1993) *Proc. Natl. Acad. Sci. U. S. A.* **90**, 8103–8107
52. Finazzi-Agrò, A., Avigliano, I., Veldink, G. A., Vliegthart, J. F. G., and Boldingh, J. (1973) *Biochim. Biophys. Acta* **326**, 462–470
53. O'Donnell, V. B., Eiserich, J. P., Chumley, P. H., Jablonsky, M. J., Krishna, N. R., Kirk, M., Barnes, S., Darley-Usmar, V. M., and Freeman, B. A. (1999) *Chem. Res. Toxicol.* **12**, 83–92
54. Lefer, A. M., and Ma, X. L. (1993) *Arterioscler. Thromb.* **13**, 771–776
55. Cayatte, A. J., Palacino, J. J., Horten, K., and Cohen, R. A. (1994) *Arterioscler. Thromb.* **14**, 753–759
56. Davies, M. G., Dalen, H., Kim, J. H., Barber, L., Svendsen, E., and Hagen, P. O. (1995) *J. Surg. Res.* **59**, 35–42
57. Cooke, J. P., and Tsao, P. S. (1994) *Arterioscler. Thromb.* **14**, 653–655
58. Ishiropoulos, H., Zhu, L., and Beckman, J. S. (1992) *Arch. Biochem. Biophys.* **289**, 446–451
59. Lewis, R. S., Tamir, S., Tannenbaum, S. R., and Deen, W. M. (1995) *J. Biol. Chem.* **270**, 29350–29355
60. Egmond, M. R., Fasella, P. M., Veldink, G. A., Vliegthart, J. F. G., and Boldingh, J. (1977) *Eur. J. Biochem.* **76**, 469–479
61. Ludwig, P., Holzhütter, H. G., Colosimo, A., Silvestrini, M. C., Schewe, T., and Rapoport, S. M. (1987) *Eur. J. Biochem.* **168**, 325–337
62. Gallon, A. A., and Pryor, W. A. (1993) *Lipids* **28**, 125–133
63. Gallon, A. A., and Pryor, W. A. (1994) *Lipids* **29**, 171–176
64. Stone, J. R., and Marletta, M. A. (1996) *Biochemistry* **35**, 1094–1099